Technical Notes

TECHNICAL NOTES are short manuscripts describing new developments or important results of a preliminary nature. These Notes cannot exceed 6 manuscript pages and 3 figures; a page of text may be substituted for a figure and vice versa. After informal review by the editors, they may be published within a few months of the date of receipt. Style requirements are the same as for regular contributions (see inside back cover).

Flight Test Base Pressure Results for Sharp 8° Cones

RICHARD G. BATT*
TRW Systems Group, Redondo Beach, Calif.

1. Introduction

ANALYTIC studies of the hypersonic near wake problem often make use of base pressure measurements and resulting correlations in order to verify and/or upgrade calculated results. Although an extensive amount of base pressure data have been obtained from wind-tunnel test experiments only a limited amount of results are available for interference free data under high Mach number conditions.[1-3] In addition, because available flight test data on base pressures have been obtained with pressure gages whose full scale ranges were 0.1 psia or greater, published results on flight test base pressures[4-8] correspond primarily to moderate or high Reynolds number conditions. The purpose of the present Note is to present additional base pressure results obtained through use of low range gages (0.01 and 0.05 psia full scale) on three conical flight vehicles of 8° half angle. These data represent a set of unique flight test base pressure measurements extending to low Reynolds number and are shown herein along with other results, also previously unpublished, for 8° half-angle conical vehicles as obtained through use of 0.1, 1.0 and 2.0 psia gages. All data correspond to zero angle-of-attack conditions at a freestream Mach number of ($M_\infty \simeq$)20. Results are available for three types of heatshield material which can be categorized as high, medium, and nonablators corresponding to turbulent mass loss parameters of [$(\dot{m}/\rho A v)_T \simeq$] 0.05, 0.01, and 0.0, respectively. Taken together, the complete set of data represents a composite summary of flight test base pressure data for 8° half-angle cone vehicles covering a range of Reynolds number of ($Re_{\infty L} \simeq$) 2×10^5 to 3×10^8.

2. Experimental Technique

The low range data discussed herein were measured through use of dual range gages which were located for each vehicle at a radial location of ($r/R =$) 0.54. For this stretched diaphragm gage the dual output feature was accomplished through use of two amplifiers which independently provided 5 v d.c. outputs at pressure levels of 0.01 psia and 0.05 psia. Response time tests and analyses determined that a small (10%) bias correction to the local raw data was appropriate in order to account for time lag effects associated with the pressure gage assembly. This correction has therefore been applied to all the low range data presented herein. Since final results have been validated to ±5% full scale, only data greater than 5% full scale are presented.

The data obtained with the 0.1, 1.0, and 2.0 psia gages, as shown herein, correspond to results which were 10% full scale or greater. Data are presented for each of three radial locations ($r/R = 0$, 0.33, and 0.46) and for the three mass loss parameters previously described. The noted results were determined from measured pressure data as documented in appropriate flight test reports. All told, a total of 13 sets (flights) of validated data were reduced in order to satisfactorily complete the present correlation study. Response time corrections have not been applied to these data since time lag effects were minimized as a result of the high absolute level of measured pressures.

3. Results

Figure 1 presents a composite set of results from the present correlation study in terms of normalized pressure data as a function of freestream Reynolds number based on vehicle wetted length. All results as shown represent zero angle-of-attack data for 8° half-angle cone vehicles with rounded shoulders ($0.167 \leq r_s/R_B \leq 0.333$) and bluntness ratios less than 0.02. The noted data were generated through use of freestream pressures of Ref. 9 and "smoothed" radar tracking trajectories. Figures 1a–c correspond to data with turbulent mass loss parameters of [$(\dot{m}/\rho A v)_T \simeq$] 0.05, 0.01, and 0, respectively. Since base pressure results for radial locations of ($r/R =$) 0 and 0.36 (high pressure gages only) were available for several flights of each heatshield material, these data are presented through use of crosshatched bands instead of symbols as a means to summarize the collected results for several flights.

The usefulness of the current low range data is evident from the extension of the measured base pressure distribution for these 8° conical vehicles to significantly lower Reynolds numbers. The present low range data have already been of use in studies of laminar near wake phenomena especially in predicting basic flowfield characteristics. Typical of these studies is the analytical treatment of the near wake by Ohrenberger and Baum.[10,11] One result from their method for a nonablating 8° cone gives a base pressure at $Re_{\infty L} = 4 \times 10^6$ which agrees favorably with the flight data. This is shown in Fig. 1c, and superimposed on it with good agreement with the data is the predicted rate of change of base pressure with $Re_{\infty L}$ for an ideal gas flow from Ref. 11. As expected with regard to these high altitude data, negligible dependence on turbulent mass loss parameter is evident for those low Reynolds numbers where the degree of heatshield ablation is negligible. Also all results indicate that the base pressure approaches a maximum with decreasing Reynolds number in a manner similar to that found by Van Hise[12] and Kavanau.[13] Interestingly enough, the "maximizing" Reynolds number ($1 - 2 \times 10^5$) is comparable to that found by the latter authors even though their results correspond to two-dimensional and axisymmetric bodies in supersonic flow. Although not shown by the current fixed-location data, a pronounced radial gradient in base pressure has been observed at low Reynolds number as evidenced by the data of Cassento[6] in Fig. 1c. This gradient tends to become small for Reynolds number approaching boundary-layer transition. This latter effect was found to be the case for the results obtained with 0.1 psia pressure gages and thus no distinction between radial locations of ($r/R =$) 0 and 0.36 has been made in Fig. 1 for those data near transition. It can also be seen that the results from Ref. 6 for $\theta/2 = 10°$ compare favorably with the present low range data when correlated in terms of freestream properties. Such satisfactory agreement between data for slender cones differing slightly in half-angle is consistent with findings from a study of wedge base pressures at $M_\infty = 6$ (Ref. 14). In addition, this favorable comparison suggests that freestream pressure and Reynolds number represent approximate scaling parameters for slender cone base pressures at least for cases where differences in cone half angles are small.

Received April 2, 1973; revision received September 24, 1973.
Index categories: Jets, Wakes, and Viscid-Inviscid Flow Interactions; Supersonic and Hypersonic Flow.

* Staff Engineer, Fluid Mechanics Laboratory. Member AIAA.

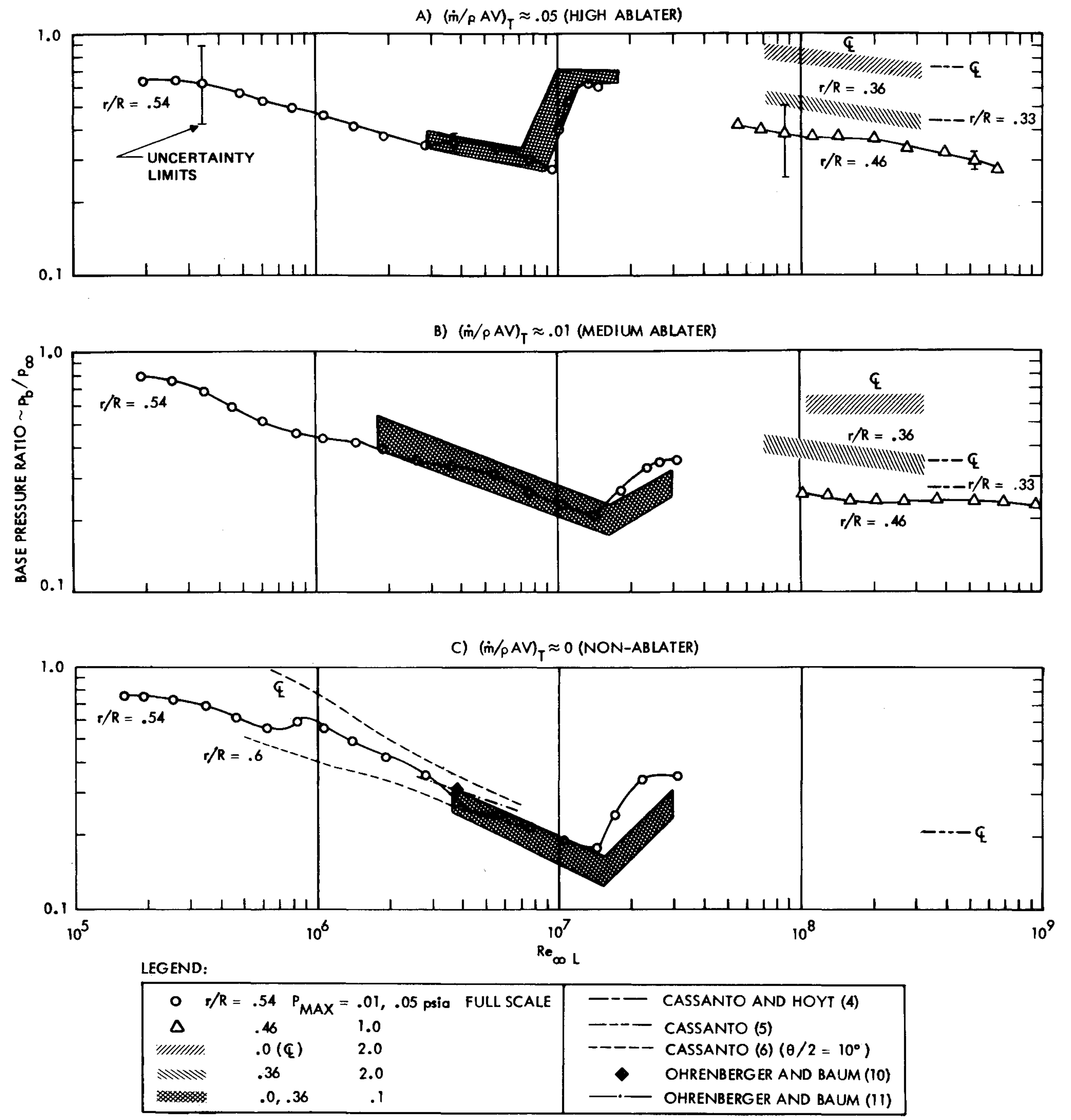

Fig. 1 Base pressure summary—flight test results for 8° half-angle cones.

A primary base pressure characteristic is the Reynolds number at which the base pressure exhibits a sharp deviation from its laminar near wake behavior. It can be seen from Fig. 1 that general agreement exists between the data for a given heatshield material with regard to the "transition" Reynolds number even though differences between heatshield types are in evidence as also observed by Cassanto and Hoyt.[4] With the onset of boundary-layer transition, the shoulder boundary-layer thickness experiences a relatively sudden increase which in turn causes a corresponding increase in the vehicle's normalized base pressure. This dependence of base pressure on boundary-layer thickness was originally pointed out by Chapman[15] and additionally verified by other investigators.[14] The sharp breakaway behavior in base pressure at transition is representative of the initiation of fully turbulent flow for the cone boundary layer which occurs at a somewhat higher Reynolds number than the onset of transitional flow phenomena.[8]

The low altitude data for the present correlation are shown to the right of Figs. 1a and 1b. Unfortunately, instrumentation difficulties prevented the acquisition of low altitude data for the nonablating heatshield vehicles (Fig. 1c). A distinct radial gradient in base pressure is evidenced by the available data, a feature of ablating heatshields under turbulent conditions also recognized by Cassanto and Hoyt.[4] Estimated turbulent pressure levels are also indicated in Fig. 1 from previous correlation studies of Refs. 4 and 5. These estimates are seen to be low for the 0.01 data but are quite favorable for the data corresponding to a mass loss parameter of 0.05.

References

[1] Iannuzi, F. A. and Weddington, E. D., "Free Flight Pressure across the Base of Sharp and Blunt 10-degree Cones at Mach Numbers from 15 to 20," TR 66-223, Dec. 1966, Arnold Engineering Development Center, Tullahoma, Tenn.

[2] Softley, E. J. and Graber, B. C., "An Experimental Study of the Pressure and Heat Transfer on the Base of Cones in Hypersonic Flow," AGARD, CP 19, May 1967.

[3] Murman, E. M., "Experimental Studies of a Laminar Hypersonic Cone Wake," *AIAA Journal*, Vol. 7, No. 9, Sept. 1969, pp. 1724–1730.

[4] Cassanto, J. M. and Hoyt, T. L., "Flight Results Showing the Effect of Mass Addition on Base Pressure," *AIAA Journal*, Vol. 8, No. 9, Sept. 1970, pp. 1705–1707.

[5] Cassanto, J. M., "Flight Test Base Pressure Results at Hypersonic Mach Numbers in Turbulent Flow," *AIAA Journal*, Vol. 10, No. 3, March 1972, pp. 329–331.

[6] Cassanto, J. M., "Radial Base Pressure Gradients in Laminar Flow," *AIAA Journal*, Vol. 5, No. 12, Dec. 1967, pp. 2278–2279.

[7] Cassanto, J. M., "Ratio on Base Pressure," *AIAA Journal*, Vol. 3, No. 12, Dec. 1965, pp. 2351–2352.

[8] Sherman, M. M. and Nakumura, T., "Flight Test Measurements of Boundary Layer Transition on a Non-Ablating 22° Cone," *Journal of Scientific Research*, Vol. 7, No. 2, Feb. 1970, pp. 137–142.

[9] *U.S. Standard Atmospheric Supplements*, 1966, 15° N. Annual.

[10] Ohrenberger, J. T. and Baum, E., "Laminar Near Wake Solutions under Atmospheric Entry Conditions," AIAA Paper 72-116, San Diego, Calif., 1972.

[11] Ohrenberger, J. T. and Baum, E., "A Theoretical Model of the Near Wake of a Slender Body in Supersonic Flow," *AIAA Journal*, Vol. 10, No. 9, Sept. 1972, pp. 1165–1172.

[12] Van Hise, V., "Investigation of Variation in Base Pressure over the Reynolds Number Range in which Wake Transition Occurs for Two-Dimensional Bodies at Mach Numbers from 1.95 to 2.92," TN D-167, Nov. 1959, NASA.

[13] Kavanau, L. L., "Results of Some Based Pressure Experiments at Intermediate Reynolds Numbers with $M = 2.84$," *Journal of Aerospace Sciences*, Vol. 21, April 1954; also "Base Pressure Studies in Rarefied Supersonic Flows," Preprint 529, Jan. 1955, Institute of Aerospace Sciences,

[14] Batt, R. G. and Kubota, T., "Experimental Investigation of Laminar Near Wakes behind 20° Wedges at $M_\infty = 6$," *AIAA Journal*, Vol. 6, No. 11, Nov. 1968, pp. 2077–2083.

[15] Chapman, D. R., "An Analysis of Base Pressure at Supersonic Velocities and Comparison with Experiment," Rept. 1051, May 1950, NACA.

Concerning Lateral Dynamics of Flight on a Great Circle

JOHN E. COCHRAN JR.*
Auburn University, Auburn, Ala.

Introduction

IN a fairly recent paper, Drummond[1] considered the lateral stability of a hypersonic vehicle, representative of a space shuttle or hypersonic transport, which was flying above the Earth in a great circle. He obtained a set of six, coupled, linear differential equations with constant coefficients which govern the perturbed motion of such a vehicle.

The characteristic equation associated with the linear system of Ref. 1 is the product of quartic and quadratic factors. The roots of the quadratic factor are complex conjugates with zero real parts and hence together represent an undamped oscillatory mode. The periodic motion in this mode is a phenomenon not predicted by results of conventional stability studies which utilize a flat-Earth model and a rectilinear reference flight path.

In this Note, a simple transformation of one of Drummond's dependent variables is made with the result that the dynamics of the perturbed lateral motion are uncoupled from the kinematics of the flight path. That is, the transformation allows one to separate the governing equations into two sets of equations, one of fourth order (dynamic equations) and one of second order (kinematic equations). The dynamic equations are uncoupled from the kinematic equations, but not the converse. As such, the equations obtained here are very similar to those obtained using a flat-Earth model.[2] The principal difference is that the two kinematic equations are coupled and when perturbations in the dynamic variables vanish, the kinematic equations yield the undamped oscillatory motion cited in Ref. 1. Furthermore, the modified equations presented here allow an interesting physical interpretation of the new oscillatory mode to be made.

Analysis

If the variable,† $\chi = \phi - \bar{y}_1$ (see Fig. 1), (where ϕ is the roll perturbation angle of the vehicle, $\bar{y}_1 = y_1/R_e$, y_1 is the lateral displacement of the center of mass of the vehicle and R_e is the radius of the Earth) is introduced into Eqs. (14–19) of Ref. 1, then the following two sets of equations may be obtained:

$$d\chi/d\hat{t} = (L/b)\hat{p} - (L/2R_e)\cos\phi_o\beta \tag{1a}$$

$$2\mu(d\beta/d\hat{t}) = C_{y_\beta}\beta + C_{y_p}\hat{p} + (C_{y_r} - 2\mu L/b)\hat{r} + C_W\cos\phi_o\chi \tag{1b}$$

$$\begin{aligned} D(d\hat{p}/d\hat{t}) = {} & (i_C C_{l_\beta} + i_E C_{n_\beta})\beta + \\ & [i_C C_{l_p} + i_E C_{n_p} + 2\hat{Q}_o(L/b)^2 i_E(i_A - i_B + i_C)]\hat{p} + \\ & \{i_C C_{l_r} + i_E C_{n_r} + 2\hat{Q}_o(L/b)^2[i_C(i_B - i_C) - i_E{}^2]\}\hat{r} \end{aligned} \tag{1c}$$

$$\begin{aligned} D(d\hat{r}/d\hat{t}) = {} & (i_A C_{n_\beta} + i_E C_{l_\beta})\beta + \\ & \{i_A C_{n_p} + i_E C_{l_p} + 2\hat{Q}_o(L/b)^2[i_A - i_B + i_E{}^2]\}\hat{p} + \\ & \{i_A C_{n_r} + i_E C_{l_r} + 2\hat{Q}_o(L/b)^2[i_B - i_A - i_C]i_E\}\hat{r} \end{aligned} \tag{1d}$$

where

$$D = 2(L/b)^2(i_A i_C - i_E{}^2)$$

and

$$d\psi/d\hat{t} + (L/2R_e)\bar{y}_1 = -(L/2R_e)\chi + (L/b)\cos\phi_o\hat{r} \tag{2a}$$

$$d\bar{y}_1/d\hat{t} - (L/2R_e)\psi = (L/2R_e)\cos\phi_o\beta \tag{2b}$$

In Eqs. (1) and (2), β is the side-slip angle, $\hat{p}$ and $\hat{r}$ are the x- and z-components‡ (roll and yaw) of the perturbation in the vehicle's angular velocity, and ψ is the perturbation in the vehicle's yaw angle. Also, $\hat{Q}_o = -L\cos\phi_o/2R_e$, where L is the

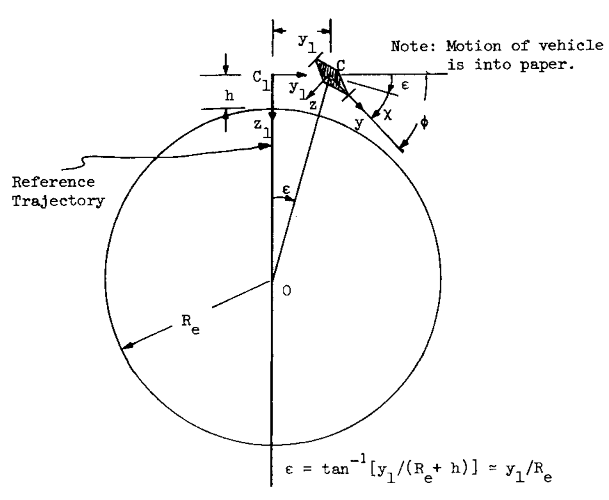

Fig. 1 Definition of the angle χ.

Received June 20, 1973; revision received October 12, 1973.

Index categories: Aircraft Handling, Stability, and Control; Entry Vehicle Dynamics and Control.

* Assistant Professor, Department of Aerospace Engineering. Member AIAA.

† The angle χ is the roll angle of the vehicle with respect to a "perturbed" great circle.

‡ Stability axes were used in deriving the original equations.